A MIXED FINITE ELEMENT FORMULATION BASED ON THE REISSNER-MINDLIN PLATE THEORY FOR A MOVING ORTHOTROPIC THIN PLATE

Project F006

FINAL REPORT

to the

Papermaking Project Advisory Committee

of the

Institute of Paper Science and Technology

December 1997

Institute of Paper Science and Technology
500 10th Street, N.W.
Atlanta, GA 30318

A MIXED FINITE ELEMENT FORMULATION BASED ON THE REISSNER-MINDLIN PLATE THEORY FOR A MOVING ORTHOTROPIC THIN PLATE

Project F006

F I N A L R E P O R T

to the

Papermaking Project Advisory Committee

of the

Institute of Paper Science and Technology

by

Xiaodong Wang, Ph.D.

December 1997

A Mixed Finite Element Formulation Based on the Reissner-Mindlin Plate Theory for a Moving Orthotropic Thin Plate

by

Xiaodong Wang, Assistant Professor of Engineering
Institute of Paper Science and Technology
500 10th Street, N.W., Atlanta, GA 30318

Abstract

With the increase of machine speeds in paper, thin film, and textile manufacturing processes, the vibration and instability of the traveling web and the web release from roll surfaces have received much attention. To couple with the experimental investigation, a reliable numerical procedure is often needed in modeling static and dynamic behaviors of three-dimensional moving sheets. The development of this reliable formulation for orthotropic moving paper sheets is the key to further investigations of edge flutter and web stress analysis.

A mixed finite element formulation based on the Reissner-Mindlin plate theory is developed and implemented for a moving orthotropic thin plate. The finite element interpolations are selected according to MITC (mixed interpolated tensorial components) plate bending elements, which have recently been proven to satisfy, numerically, the inf-sup condition. We show, with a few test cases, that the proposed formulation is reliable for both frequency and transient dynamics analyses, and that no shear locking is encountered.

1 Introduction

In the paper, textile, plastic film, and other industries involving moving thin materials, stress analysis is essential for the control of wrinkle, flutter, and sheet break. Similar vibration problems of moving plate and shell structures can also be found in aeronautic and aerospace structures, computer hard disk drives, and rotating blades in turbomachinery. Although the mechanical behavior of axially moving materials, in general, has been studied for many years, little information is available on the stress analysis of moving thin materials. Following the early work of Mote [18], significant research efforts have been directed toward studying the linear and nonlinear dynamical behavior of an axially moving string model [31] [32] [33]. Furthermore, in order to consider the dynamical behavior of moving materials coupled with surrounding fluid/air, in practice, one often ignores boundary layer shear forces and introduces different added mass expressions for the Coriolis and centrifugal inertia terms [21]. For the purpose of attenuation and guidance, coupling problems between moving material and fluid/air bearings have also been studied [20] [25] [29] [34]. More recently, Heinrich and Connolly [11] carried out a three-dimensional analysis of an axially moving tape coupled with bearings, by using the classical Kirchhoff thin plate assumptions [11]. However, it has been indicated in Ref. [30] that when the axial tension is not predominant, the so-called shear locking phenomena need to be avoided. This suggests that in order to predict accurately the transverse shear, as well as in-plane stress distributions of the moving thin plate and shell structures, reliable numerical formulations are needed. The importance and practical applications of such work were discussed by Lee and Ng [16], where they applied a mode method with the Kirchhoff thin plate theory for isotropic materials and Lagrangian kinematic descriptions to avoid convective terms; However, no work

has been documented in predicting the stress distributions of moving orthotropic thin plates.

Since the inception of finite element methods, many plate bending formulations and elements have been investigated; proper review of such topics is available in Refs. [1] [13] [23] [24]. It has been widely recognized that mixed plate formulation based on the Reissner-Mindlin theory can effectively eliminate "shear locking" and predict accurately and reliably stress levels of thin plates [4] [5] [9]. Recently, the MITC elements have been proven, numerically, to satisfy the inf-sup condition [14]. The basic difficulty in choosing proper orders of interpolation for out-of-plane displacement, section rotations, and transverse shear strains which result in nonlocking behavior and optimal convergence of the element is summarized in Refs. [3] [4] [5].

The purpose of this paper is to extend the mixed plate formulation, based on the Reissner-Mindlin theory with MITC elements, to the analyses of axially moving orthotropic thin plates. In the following sections, we first briefly summarize the mathematical models, the corresponding assumptions, and the governing equations. Next, we present the mixed finite element formulation and some generic numerical examples. Although no mathematical theory is available to prove rigorously that with the incorporation of the axial motion, and consequently the loss of the coerciveness due to gyroscopic inertia terms, the proposed formulation with MITC elements is reliable as it is for the case of stationary plates and shells, we employ test examples for both frequency and transient dynamics analyses to confirm, numerically, the reliability and accuracy of the proposed formulation for moving orthotropic thin plates.

2 Plate Displacement, Strain, and Stress

In a three-dimensional elasticity theory, there are six stress components that are expressed in terms of six strain components through material constitutive laws. For the general plate section illustrated in Fig. 1, the top and bottom faces of the plate (at $z = \pm d/2$) are considered to be free from tangential traction, but under normal pressures p^+ and p^-, i.e.,

$$\begin{array}{rclrcl} \tau_{xz}|_{z=\pm d/2} & = & 0, & \tau_{yz}|_{z=\pm d/2} & = & 0; \\ \tau_{zz}|_{z=+d/2} & = & -p^+, & \tau_{zz}|_{z=-d/2} & = & -p^-. \end{array} \tag{1}$$

For convenience, we set $p = p^- - p^+$. We recognize that in some cases we may have to modify the above assumptions concerning the surrounding air shear boundary layer.

Corresponding to the five stress components, the bending and twisting moments, and the transverse shearing forces, all measured per unit of length, are defined as

$$(M_x, M_y, M_{xy}) = \int_{-d/2}^{+d/2} (\tau_{xx}, \tau_{yy}, \tau_{xy}) z dz, \tag{2}$$

$$(Q_x, Q_y) = \int_{-d/2}^{+d/2} (\tau_{xz}, \tau_{yz}) dz. \tag{3}$$

Also shown in Fig. 1, $\boldsymbol{\beta} = (\beta_x, \beta_y)$ is the vector whose components are, respectively, the rotations of the normal to the undeformed middle surface in the x,z and y,z planes; it is equivalent to $\boldsymbol{\theta}^\perp = (-\theta_y, \theta_x)$, which is normal to the vector $\boldsymbol{\theta}$ of rotations about the Cartesian axes x and y. In the classical Kirchhoff plate theory, the transverse strains and stresses are ignored and, consequently, $\nabla w = \boldsymbol{\beta}$. However, we assume in this paper, according to the Reissner-Mindlin plate theory [17]

[22], that the x-direction and y-direction displacements u and v are proportional to z, and that the z-direction displacement w is independent of z, i.e.,

$$u = -z\beta_x(x,y,t), \quad v = -z\beta_y(x,y,t), \quad w = w(x,y,t). \tag{4}$$

Moreover, the five strain components are introduced as follows:

$$\begin{bmatrix} \epsilon_{xx} \\ \epsilon_{yy} \\ \gamma_{xy} \end{bmatrix} = -z \begin{bmatrix} \dfrac{\partial \beta_x}{\partial x} \\ \dfrac{\partial \beta_y}{\partial y} \\ \dfrac{\partial \beta_x}{\partial y} + \dfrac{\partial \beta_y}{\partial x} \end{bmatrix} = -z\boldsymbol{\kappa}, \quad \begin{bmatrix} \gamma_{xz} \\ \gamma_{yz} \end{bmatrix} = \begin{bmatrix} \dfrac{\partial w}{\partial x} - \beta_x \\ \dfrac{\partial w}{\partial y} - \beta_y \end{bmatrix} = \boldsymbol{\gamma}. \tag{5}$$

In general, for an orthotropic material, we have

$$\begin{bmatrix} \tau_{xx} \\ \tau_{yy} \\ \tau_{xy} \end{bmatrix} = \begin{bmatrix} a_{11} & a_{12} & 0 \\ a_{21} & a_{22} & 0 \\ 0 & 0 & a_{33} \end{bmatrix} \begin{bmatrix} \epsilon_{xx} \\ \epsilon_{yy} \\ \gamma_{xy} \end{bmatrix} = -\mathbf{C}_\epsilon z\boldsymbol{\kappa} \tag{6}$$

$$\begin{bmatrix} \tau_{xz} \\ \tau_{yz} \end{bmatrix} = \begin{bmatrix} a_{44} & 0 \\ 0 & a_{55} \end{bmatrix} \begin{bmatrix} \gamma_{xz} \\ \gamma_{yz} \end{bmatrix} = \mathbf{C}_\gamma \boldsymbol{\gamma} \tag{7}$$

where the material constants are defined by

$$a_{11} = \frac{E_x}{1-\nu_{xy}\nu_{yx}}, \quad a_{12} = a_{21} = \frac{\nu_{xy}E_x}{1-\nu_{xy}\nu_{yx}}, \quad a_{22} = \frac{E_y}{1-\nu_{xy}\nu_{yx}}; \tag{8}$$

$$a_{33} = G_{xy}, \quad a_{44} = G_{xz}, \quad a_{55} = G_{yz}. \tag{9}$$

In addition to the usual necessary condition $\dfrac{E_x}{\nu_{yx}} = \dfrac{E_y}{\nu_{xy}}$, for paper materials, we also have the Campbell relationship $\dfrac{1}{G_{xy}} = \dfrac{1+\nu_{yx}}{E_x} + \dfrac{1+\nu_{xy}}{E_y}$ [6]. Of course, in the

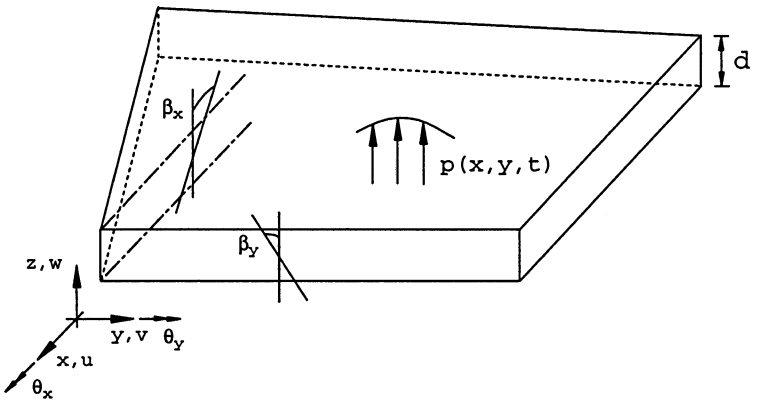

Figure 1: Plate deformation assumptions including transverse shear.

case of an isotropic material, we would have $E_x = E_y = E$, $\nu_{xy} = \nu_{yx} = \nu$, and $G_{xy} = G_{xz} = G_{yz} = \dfrac{E}{2(1+\nu)}$.

Substituting Eqs. (6) and (7) into Eqs. (2) and (3), we obtain

$$M_x = -(a_{11}\frac{\partial \beta_x}{\partial x} + a_{12}\frac{\partial \beta_y}{\partial y})\frac{d^3}{12} \tag{10}$$

$$M_y = -(a_{21}\frac{\partial \beta_x}{\partial x} + a_{22}\frac{\partial \beta_y}{\partial y})\frac{d^3}{12} \tag{11}$$

$$M_{xy} = -a_{33}(\frac{\partial \beta_x}{\partial y} + \frac{\partial \beta_y}{\partial x})\frac{d^3}{12} \tag{12}$$

and

$$Q_x = kd(\frac{\partial w}{\partial x} - \beta_x)a_{44} \tag{13}$$

$$Q_y = kd(\frac{\partial w}{\partial y} - \beta_y)a_{55}. \tag{14}$$

The constant k plays a role in accounting for the nonuniform distribution of transverse shear stresses through the plate thickness, and has the value 5/6 in this

paper. A more elaborate discussion with regard to the selection of k is available in Refs. [2] [17].

3 Governing Equations

From the force equilibrium equations, i.e., $\tau_{ij,j} + f_i = \rho \frac{d^2 u_i}{dt^2}$, where f_i is the body force; ρ is the mass density; and the indices i ($i = 1, 2, 3$) represent the x, y, and z directions, we obtain

$$\frac{\partial M_x}{\partial x} + \frac{\partial M_{xy}}{\partial y} - Q_x = -\frac{\rho d^3}{12}\frac{d^2\beta_x}{dt^2} \quad (15)$$

$$\frac{\partial M_{xy}}{\partial x} + \frac{\partial M_y}{\partial y} - Q_y = -\frac{\rho d^3}{12}\frac{d^2\beta_y}{dt^2} \quad (16)$$

$$\frac{\partial Q_x}{\partial x} + \frac{\partial Q_y}{\partial y} + p - \rho g d = \rho d \frac{d^2 w}{dt^2}. \quad (17)$$

Of course, as indicated in Eq. (17), the only body force considered in this paper is the gravitational force in the negative z direction. Furthermore, in terms of out-of-plane displacement w, and two rotations β_x and β_y, we obtain from Eqs. (10) to (14)

$$a_{11}\frac{\partial^2\beta_x}{\partial x^2} + a_{12}\frac{\partial^2\beta_y}{\partial x\partial y} + a_{33}\frac{\partial^2\beta_x}{\partial y^2} + a_{33}\frac{\partial^2\beta_y}{\partial x\partial y} + a_{44}(\frac{\partial w}{\partial x} - \beta_x)\frac{12k}{d^2} = \rho\frac{d^2\beta_x}{dt^2} \quad (18)$$

$$a_{33}\frac{\partial^2\beta_x}{\partial x\partial y} + a_{33}\frac{\partial^2\beta_y}{\partial x^2} + a_{21}\frac{\partial^2\beta_x}{\partial x\partial y} + a_{22}\frac{\partial^2\beta_y}{\partial y^2} + a_{55}(\frac{\partial w}{\partial y} - \beta_y)\frac{12k}{d^2} = \rho\frac{d^2\beta_y}{dt^2} \quad (19)$$

$$a_{44}(\frac{\partial^2 w}{\partial x^2} - \frac{\partial\beta_x}{\partial x})k + a_{55}(\frac{\partial^2 w}{\partial y^2} - \frac{\partial\beta_y}{\partial y})k + \frac{p}{d} - \rho g = \rho\frac{d^2 w}{dt^2}. \quad (20)$$

We note here that when the plate is stationary, the material derivative $\frac{d}{dt}$ is the same as the spatial derivative $\frac{\partial}{\partial t}$; however, when the plate is moving with velocity

V in the x direction, we have $\frac{d}{dt} = \frac{\partial}{\partial t} + V\frac{\partial}{\partial x}$. In general, for moving materials, we have $\frac{d}{dt} = \frac{\partial}{\partial t} + \mathbf{V} \cdot \boldsymbol{\nabla}$.

For an isotropic and stationary plate without the gravitational force, the following governing equations presented by Mindlin [17] are recovered,

$$\frac{D}{2}[(1-\nu)\nabla^2\beta_x + (1+\nu)\frac{\partial\phi}{\partial x}] + kGd(\frac{\partial w}{\partial x} - \beta_x) = \frac{\rho d^3}{12}\frac{\partial^2\beta_x}{\partial t^2} \quad (21)$$

$$\frac{D}{2}[(1-\nu)\nabla^2\beta_y + (1+\nu)\frac{\partial\phi}{\partial y}] + kGd(\frac{\partial w}{\partial y} - \beta_y) = \frac{\rho d^3}{12}\frac{\partial^2\beta_y}{\partial t^2} \quad (22)$$

$$kGd(\nabla^2 w - \phi) + p - \rho g d = \rho d\frac{\partial^2 w}{\partial t^2} \quad (23)$$

where ϕ is defined as $\frac{\partial\beta_x}{\partial x} + \frac{\partial\beta_y}{\partial y}$, and the bending stiffness D equals $\frac{Ed^3}{12(1-\nu^2)}$. Furthermore, the classical theory of stationary isotropic elastic thin plates based on the Kirchhoff assumptions (refer to [26]) yields

$$D\nabla^4 w + \rho d\frac{\partial^2 w}{\partial t^2} = p - \rho g d. \quad (24)$$

It was found by Timoshenko [27], Uflyand [28], Hencky [12], and Mindlin [17] that Eq. (24) cannot be used to predict sharp transients or frequencies of high-order vibrational modes, and in order to predict such effects, transverse shear deformations have to be included.

Based on the classical Kirchhoff assumptions, for a moving isotropic thin plate with tension T, Eq. (24) is modified as

$$D\nabla^4 w + \rho d(\frac{\partial}{\partial t} + V\frac{\partial}{\partial x})^2 w - T\frac{\partial^2 w}{\partial x^2} = p - \rho g d \quad (25)$$

and this equation has been introduced in the analysis of moving tapes, saw bands, and plastic films [15] [11] [19], and the subsonic panel flutter problems [8]. Nevertheless, it has been recently recognized that if the axial tension is not predominant

or as the axial moving speed increases, spurious lateral displacements are observed [30]. This suggests that a reliable mixed plate theory is needed to predict accurately the stress distributions within a moving thin plate.

4 Mixed Plate Formulation

In the mixed formulation based on the Reissner-Mindlin plate theory, we account for the effects of inertia, by applying the Hamilton's principle with the following definition of the kinetic energy,

$$\int_{\Omega} \{\frac{\rho d^3}{24}(\frac{d\beta_x}{dt})^2 + \frac{\rho d^3}{24}(\frac{d\beta_y}{dt})^2 + \frac{\rho d}{2}(\frac{dw}{dt})^2\} d\Omega \tag{26}$$

where Ω represents the midsurface area. In actuality, we include in the body forces the following inertia terms

$$\rho d(\frac{\partial}{\partial t} + V\frac{\partial}{\partial x})^2 w, \quad \frac{\rho d^3}{12}(\frac{\partial}{\partial t} + V\frac{\partial}{\partial x})^2 \boldsymbol{\beta}. \tag{27}$$

Defining the spaces $\Theta = (H_0^1(\Omega))^2$ and $W = H_0^1(\Omega)$, and assuming that a force function f_w is given in $L^2(\Omega)$, and a moment function $\boldsymbol{f}_\beta$ is given in $(L^2(\Omega))^2$, our problem can be presented as follows:

$$\inf_{\boldsymbol{\beta}\in\Theta, w\in W} \frac{d^3}{2} a(\boldsymbol{\beta}, \boldsymbol{\beta}) + \frac{kd}{2}\|\boldsymbol{\beta} - \boldsymbol{\nabla} w\|_0^2 - d^3(f_w, w) - d^3(\boldsymbol{f}_\beta, \boldsymbol{\beta}) \tag{28}$$

where the body forces (or moments) have the form

$$f_w = (p - \rho g d - \rho d(\frac{\partial}{\partial t} + V\frac{\partial}{\partial x})^2 w)/d^3 \tag{29}$$

$$\boldsymbol{f}_\beta = -\frac{\rho}{12}(\frac{\partial}{\partial t} + V\frac{\partial}{\partial x})^2 \boldsymbol{\beta} \tag{30}$$

and the bending strain energy $\frac{d^3}{2}a(\boldsymbol{\beta},\boldsymbol{\beta})$, which includes the contribution of the normal stress $\sigma_T(y)$ due to the axial tension, is expressed by

$$\frac{d^3}{2}a(\boldsymbol{\beta},\boldsymbol{\beta}) = \frac{d^3}{24}\int_\Omega \boldsymbol{\kappa}^T \mathbf{C}_\epsilon \boldsymbol{\kappa} d\Omega + \int_\Omega \frac{d\sigma_T(y)}{2}(\frac{\partial w}{\partial x})^2 d\Omega. \tag{31}$$

Given the finite element subspaces $\Theta_h \subset \Theta$ and $W_h \subset W$, the discretized problem may be written as

$$\inf_{\boldsymbol{\beta}_h \in \Theta_h, w_h \in W_h} \frac{d^3}{2}a(\boldsymbol{\beta}_h,\boldsymbol{\beta}_h) + \frac{kd}{2}\|R\boldsymbol{\beta}_h - \boldsymbol{\nabla} w_h\|_0^2 - d^3(f_w, w_h) - d^3(\boldsymbol{f}_\beta, \boldsymbol{\beta}_h) \tag{32}$$

where the linear operator R satisfies $R\boldsymbol{\nabla} w_h = \boldsymbol{\nabla} w_h, \forall w_h \in W_h$ and $\|R\boldsymbol{\beta}_h\|_1 \leq c\|\boldsymbol{\beta}_h\|_1, \forall \boldsymbol{\beta}_h \in \Theta_h$, and the transverse shear strains $\boldsymbol{\gamma}_h$ are expressed as $kd^{-2}(R\boldsymbol{\beta}_h - \boldsymbol{\nabla} w_h)$. Notice that the shear strain energy is given by $\frac{kd}{2}\|R(\boldsymbol{\beta}_h - \boldsymbol{\nabla} w_h)\|_0^2$ instead of $\frac{kd}{2}\|\boldsymbol{\beta}_h - \boldsymbol{\nabla} w_h\|_0^2$. In essence, the successful selection of R ensures the reliability of the mixed formulation [4] [9]. In fact, the need for such a mixed formulation is reflected in Eqs. (18) to (20), where the shear terms are predominant just as bulk modulus for almost incompressible materials [2]. When the plate is moving, as occurred during a transport process or during the rotation of blades, computer hard disks, and space structures, additional difficulties arise when the Coriolis force breaks the self-adjoint property and, moreover, along with the centrifugal force, introduces destabilizing effects.

For the limiting case in which $d \to 0$, the limit w corresponds to the Kirchhoff model, and the variational problem assumes the form

$$a(\boldsymbol{\beta}_h, \bar{\boldsymbol{\beta}}_h) + (\boldsymbol{\gamma}_h, R\bar{\boldsymbol{\beta}}_h - \boldsymbol{\nabla}\bar{w}_h) = (f_w, \bar{w}_h) + (\boldsymbol{f}_\beta, \bar{\boldsymbol{\beta}}_h), \quad \forall \bar{\boldsymbol{\beta}}_h \in \Theta_h, \forall \bar{w}_h \in W_h, \tag{33}$$

$$R\boldsymbol{\beta}_h = \boldsymbol{\nabla} w_h. \tag{34}$$

For a typical MITC4 element shown in Fig. 2, the linear operator R is selected in such a way that at the tying points (midpoints of each edge) we have $R\boldsymbol{\beta}_h = \boldsymbol{\beta}_h$ (Ref. [2]). Also as shown in Fig. 2, the angles between the r and x axes and s and x axes are defined as α and β, and the shear strains are expressed as

$$\gamma_{xz} = \gamma_{rz}\sin\beta - \gamma_{sz}\sin\alpha \tag{35}$$

$$\gamma_{yz} = -\gamma_{rz}\cos\beta + \gamma_{sz}\cos\alpha \tag{36}$$

where

$$\begin{aligned}
\gamma_{rz} &= \lambda_1\{(1+s)[\frac{w_1-w_2}{2} - \frac{x_1-x_2}{4}(\beta_x^1+\beta_x^2) - \frac{y_1-y_2}{4}(\beta_y^1+\beta_y^2)] \\
&\quad +(1-s)[\frac{w_4-w_3}{2} - \frac{x_4-x_3}{4}(\beta_x^4+\beta_x^3) - \frac{y_4-y_3}{4}(\beta_y^4+\beta_y^3)]\}/8det\mathbf{J} \\
\gamma_{sz} &= \lambda_2\{(1+r)[\frac{w_1-w_4}{2} - \frac{x_1-x_4}{4}(\beta_x^1+\beta_x^4) - \frac{y_1-y_4}{4}(\beta_y^1+\beta_y^4)] \\
&\quad +(1-r)[\frac{w_2-w_3}{2} - \frac{x_2-x_3}{4}(\beta_x^2+\beta_x^3) - \frac{y_2-y_3}{4}(\beta_y^2+\beta_y^3)]\}/8det\mathbf{J}
\end{aligned}$$

$$\mathbf{J} = \begin{bmatrix} \dfrac{\partial x}{\partial r} & \dfrac{\partial y}{\partial r} \\ \dfrac{\partial x}{\partial s} & \dfrac{\partial y}{\partial s} \end{bmatrix}$$

$$\begin{aligned}
\lambda_1 &= \sqrt{(C_x+rB_x)^2+(C_y+rB_y)^2}, & \lambda_2 &= \sqrt{(A_x+sB_x)^2+(A_y+sB_y)^2}; \\
A_x &= x_1-x_2-x_3+x_4, & A_y &= y_1-y_2-y_3+y_4; \\
B_x &= x_1-x_2+x_3-x_4, & B_y &= y_1-y_2+y_3-y_4; \\
C_x &= x_1+x_2-x_3-x_4, & C_y &= y_1+y_2-y_3-y_4.
\end{aligned}$$

For the moving plates considered in this paper, we use two built-in edge supports at $x = 0$ and $x = L$, and two free edges (zero shear forces and bending moments) at $y = 0$ and $y = B$. For the mixed thin plate theory, general specific boundary considerations are discussed in Ref. [10].

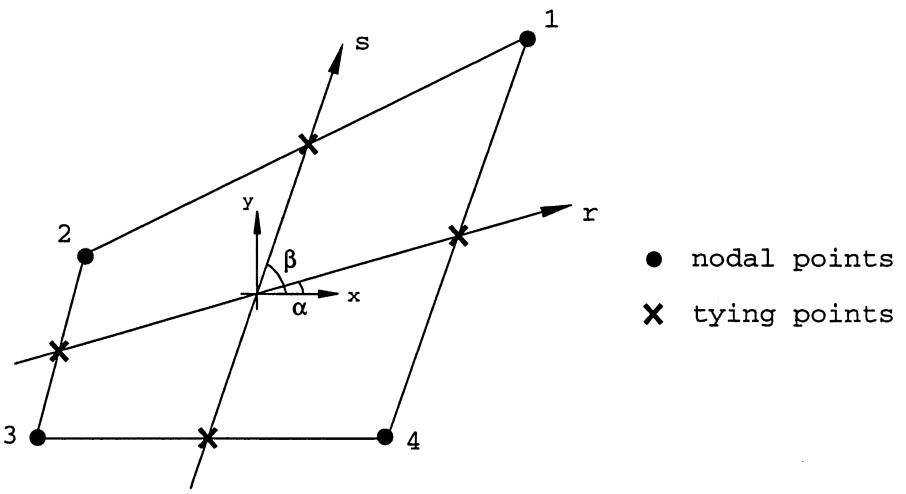

Figure 2: A general MITC4 plate element.

Using the standard procedure of interpolating, and considering a typical finite element, we have

$$w = \mathbf{H}_w\widehat{\mathbf{W}}, \quad \frac{\partial w}{\partial x} = \mathbf{B}_w\widehat{\mathbf{W}}, \quad R\boldsymbol{\beta} - \boldsymbol{\nabla} w = \mathbf{B}_{\gamma w}\widehat{\mathbf{W}} + \mathbf{B}_{\gamma x}\widehat{\boldsymbol{\beta}}_x + \mathbf{B}_{\gamma y}\widehat{\boldsymbol{\beta}}_y$$

$$\beta_x = \mathbf{H}_x\widehat{\boldsymbol{\beta}}_x, \quad \frac{\partial \beta_x}{\partial x} = \mathbf{B}_{x1}\widehat{\boldsymbol{\beta}}_x, \quad \frac{\partial \beta_x}{\partial y} = \mathbf{B}_{x2}\widehat{\boldsymbol{\beta}}_x$$

$$\beta_y = \mathbf{H}_y\widehat{\boldsymbol{\beta}}_y, \quad \frac{\partial \beta_y}{\partial x} = \mathbf{B}_{y1}\widehat{\boldsymbol{\beta}}_y, \quad \frac{\partial \beta_y}{\partial y} = \mathbf{B}_{y2}\widehat{\boldsymbol{\beta}}_y$$

where $\mathbf{H}_w$, $\mathbf{H}_x$, and $\mathbf{H}_y$ are the interpolation matrices for w, β_x, and β_y, respectively, and the solution vector is denoted as $\widehat{\mathbf{U}} = (\widehat{\mathbf{W}}, \widehat{\boldsymbol{\beta}}_x, \widehat{\boldsymbol{\beta}}_y)^T$. The matrix equations derived from the standard Galerkin formulation yield

$$\mathbf{M}\ddot{\widehat{\mathbf{U}}} + \mathbf{C}\dot{\widehat{\mathbf{U}}} + \mathbf{K}\widehat{\mathbf{U}} = \mathbf{R} \tag{37}$$

where

$$\mathbf{M} = \begin{bmatrix} \mathbf{M}_{ww} & \mathbf{0} & \mathbf{0} \\ \mathbf{0} & \mathbf{M}_{xx} & \mathbf{0} \\ \mathbf{0} & \mathbf{0} & \mathbf{M}_{yy} \end{bmatrix}, \quad \mathbf{C} = \begin{bmatrix} \mathbf{C}_{ww} & \mathbf{0} & \mathbf{0} \\ \mathbf{0} & \mathbf{C}_{xx} & \mathbf{0} \\ \mathbf{0} & \mathbf{0} & \mathbf{C}_{yy} \end{bmatrix}$$

$$\mathbf{K} = \begin{bmatrix} \mathbf{K}_{ww} & \mathbf{K}_{wx} & \mathbf{K}_{wy} \\ \mathbf{K}_{xw} & \mathbf{K}_{xx} & \mathbf{K}_{xy} \\ \mathbf{K}_{yw} & \mathbf{K}_{yx} & \mathbf{K}_{yy} \end{bmatrix}, \quad \mathbf{R} = \begin{Bmatrix} \mathbf{R}_w \\ \mathbf{R}_x \\ \mathbf{R}_y \end{Bmatrix}$$

and

$$\begin{aligned}
\mathbf{K}_{xx} &= \int_\Omega \frac{d^3}{12}(a_{11}\mathbf{B}_{x1}^T\mathbf{B}_{x1} + a_{33}\mathbf{B}_{x2}^T\mathbf{B}_{x2})d\Omega + \int_\Omega k d\mathbf{B}_{\gamma x}^T\mathbf{C}_\gamma\mathbf{B}_{\gamma x}d\Omega - \int_\Omega \frac{\rho d^3V^2}{12}\mathbf{B}_{x1}^T\mathbf{B}_{x1}d\Omega \\
\mathbf{K}_{xy} &= \int_\Omega \frac{d^3}{12}(a_{12}\mathbf{B}_{x1}^T\mathbf{B}_{y2} + a_{33}\mathbf{B}_{x2}^T\mathbf{B}_{y1})d\Omega + \int_\Omega k d\mathbf{B}_{\gamma x}^T\mathbf{C}_\gamma\mathbf{B}_{\gamma y}d\Omega \\
\mathbf{K}_{yx} &= \int_\Omega \frac{d^3}{12}(a_{21}\mathbf{B}_{y2}^T\mathbf{B}_{x1} + a_{33}\mathbf{B}_{y1}^T\mathbf{B}_{x2})d\Omega + \int_\Omega k d\mathbf{B}_{\gamma y}^T\mathbf{C}_\gamma\mathbf{B}_{\gamma x}d\Omega \\
\mathbf{K}_{yy} &= \int_\Omega \frac{d^3}{12}(a_{22}\mathbf{B}_{y2}^T\mathbf{B}_{y2} + a_{33}\mathbf{B}_{y1}^T\mathbf{B}_{y1})d\Omega + \int_\Omega k d\mathbf{B}_{\gamma y}^T\mathbf{C}_\gamma\mathbf{B}_{\gamma y}d\Omega - \int_\Omega \frac{\rho d^3V^2}{12}\mathbf{B}_{y1}^T\mathbf{B}_{y1}d\Omega \\
\mathbf{K}_{ww} &= \int_\Omega k d\mathbf{B}_{\gamma w}^T\mathbf{C}_\gamma\mathbf{B}_{\gamma w}d\Omega + \int_\Omega (\sigma_T(y)d - \rho dV^2)\mathbf{B}_w^T\mathbf{B}_w d\Omega \\
\mathbf{R}_w &= \int_\Omega (p - \rho g d)\mathbf{H}_w^T d\Omega
\end{aligned}$$

$$\begin{aligned}
\mathbf{K}_{xw} &= \int_\Omega k d\mathbf{B}_{\gamma x}^T\mathbf{C}_\gamma\mathbf{B}_{\gamma w}d\Omega, \quad \mathbf{K}_{yw} = \int_\Omega k d\mathbf{B}_{\gamma y}^T\mathbf{C}_\gamma\mathbf{B}_{\gamma w}d\Omega; \\
\mathbf{K}_{wx} &= \int_\Omega k d\mathbf{B}_{\gamma w}^T\mathbf{C}_\gamma\mathbf{B}_{\gamma x}d\Omega, \quad \mathbf{K}_{wy} = \int_\Omega k d\mathbf{B}_{\gamma w}^T\mathbf{C}_\gamma\mathbf{B}_{\gamma y}d\Omega; \\
\mathbf{C}_{xx} &= \int_\Omega \frac{\rho d^3V}{6}\mathbf{H}_x^T\mathbf{B}_{x1}d\Omega, \quad \mathbf{C}_{yy} = \int_\Omega \frac{\rho d^3V}{6}\mathbf{H}_y^T\mathbf{B}_{y1}d\Omega; \\
\mathbf{C}_{ww} &= \int_\Omega 2\rho dV\mathbf{H}_w^T\mathbf{B}_w d\Omega, \quad \mathbf{M}_{ww} = \int_\Omega \rho d\mathbf{H}_w^T\mathbf{H}_w d\Omega; \\
\mathbf{M}_{xx} &= \int_\Omega \frac{\rho d^3}{12}\mathbf{H}_x^T\mathbf{H}_x d\Omega, \quad \mathbf{M}_{yy} = \int_\Omega \frac{\rho d^3}{12}\mathbf{H}_y^T\mathbf{H}_y d\Omega
\end{aligned}$$

and the contributions from distributed or concentrated moments in x and y directions are inclued in $\mathbf{R}_x$ and $\mathbf{R}_y$.

5 Numerical Examples

To demonstrate the capabilities and reliability of the proposed formulation based on the Reissner-Mindlin plate theory, we analyze a typical orthotropic plate (paper sheet) (depicted in Fig. 3) with the following physical parameters: $\rho = 700$ kg/m^3; $d = 0.7$ mm; $L = 2$ m; $B = 8$ m; $E_x = 7.44$ GPa; $E_y = 3.47$ GPa; $\nu_{xy} = 0.149$; $G_{xy} = 2.04$ GPa; $G_{xz} = 0.099$ GPa; $G_{yz} = 0.137$ GPa.

To evaluate the critical axial velocity of the moving plate, we have computed the first natural frequency ω with the proposed finite element formulation. It is shown in Fig. 4 that when the orthotropic plate is not under pretension, the plate bending stiffness can sustain an axial velocity up to 2 m/s. In general, the first natural frequency (flexural mode) decreases continuously with increasing axial velocity, and the lower the first natural frequency, the more susceptible the plate is to flutter. Of course, as the tension increases, the critical velocity increases as well.

Table 1 lists the results for the first five natural frequencies in the case of zero traveling velocity, and serves as one of the check points on the implemented program. As can be seen, the proposed formulation with zero axial velocity agrees exactly with the reliable Reissner-Mindlin plate theory with MITC elements in ADINA. We note that the natural frequencies computed here include the effects of transverse shear. For a stationary orthotropic thin plate which conforms to the Kirchhoff assumptions, the natural frequency approximations are available in Ref. [7].

Figure 6 shows the first two natural frequency modes for the plate moving at different velocities. In the transient dynamics analysis, we have demonstrated the flexural wave propagation in the moving plate due to an impact load calculated with the proposed formulation. The plate is subjected to an impulse force $2f(t)$ applied at the center of the plate ($x = 1$ m, $y = 4$ m). The corresponding impulse timefunction

Mode #	Frequencies (rad/sec)	
	ADINA	This Work
1	4.304	4.304
2	4.335	4.335
3	4.440	4.440
4	4.631	4.631
5	4.932	4.932

Table 1: Frequency comparison with ADINA for the zero traveling velocity case. (5×20 MITC4 plate elements).

$f(t)$ is shown in Fig. 5. The analysis is carried out for 60 time steps with step size $\Delta t = 0.02$ s. The transient response of the plate center point is presented in Fig. 7, and the MD (axial moving direction or machine direction) and CD (cross-sectional direction) displacement profiles are shown in Fig. 8 and Fig. 9, respectively. Once again, the transient response for a plate with zero velocity matches exactly with the corresponding ADINA results.

Figures 10 to 12 clearly show the Corlios and centrifugal effects associated with axial motion on the out-of-plane displacement, x-rotation, and y-rotation. No shear locking is observed in the five stress band plots in Figs. 13 to 17. The stress bands in all cases are quite smooth, indicating accurate solutions. These sets of stress band plots had not been obtained prior to the development of the mixed formulation presented here for the moving orthotropic thin plate.

6 Conclusion

The proposed mixed formulation based on the Reissner-Mindlin theory for a moving orthotropic plate is a natural extension of the reliable mixed formulation for stationary plates and shells. We consider the numerical tests used in this work to be

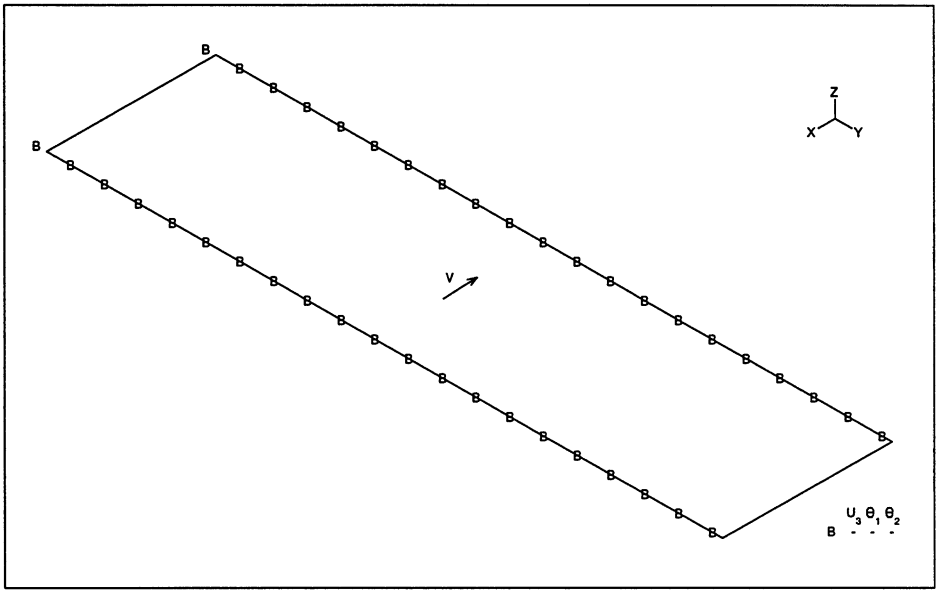

Figure 3: An orthotropic plate (2 m × 8 m) moving between two supports.

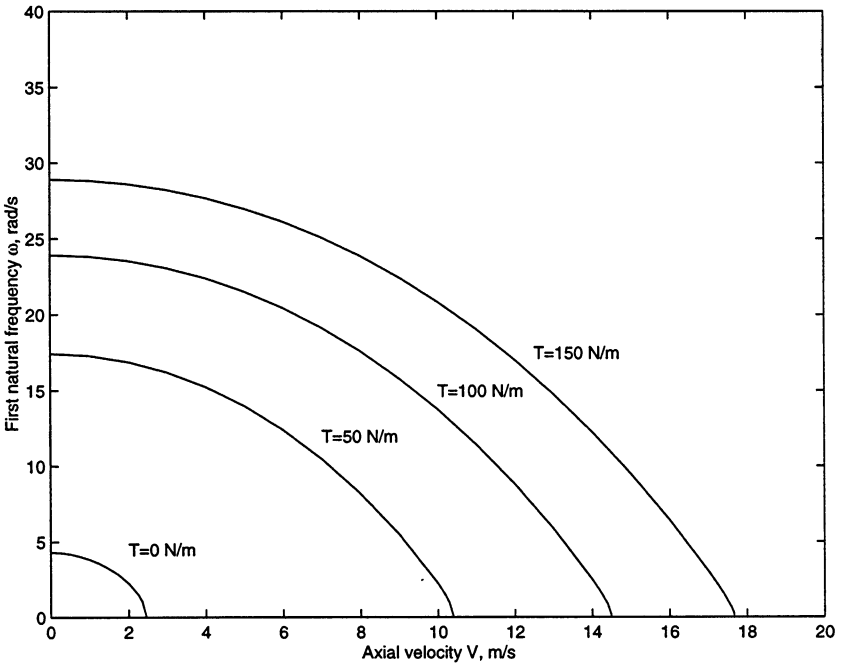

Figure 4: First natural frequency *vs.* axial velocity. (Mesh of 5 × 20 MITC4 plate elements.)

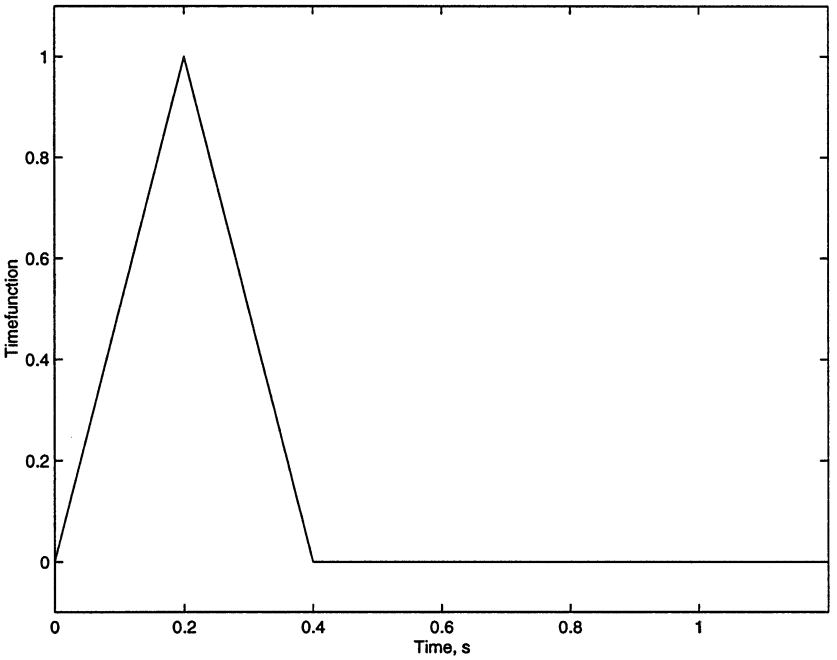

Figure 5: Impulse load timefunction $f(t)$.

comprehensive, and the natural frequencies, mode shapes, along with the five stress band plots, appear to be sufficient to exhibit deficiencies in the proposed formulation were any to exist.

The employed MITC4 plate elements are demonstrated numerically to be effective for use in the analyses of a moving orthotropic plate and other analogous problems. We also expect other MITC elements to perform similarly. A main attribute of this work is the fact that the critical axial velocity as well as the normal and shear stress waves can be predicted for any orthotropic thin plate moving at various velocities.

7 Acknowledgment

The author would like to thank the Institute of Paper Science and Technology and its Member Companies for their support, and Professor F. Bloom, Department of Mathematical Science, Northern Illinois University, for constructive comments and suggestions.

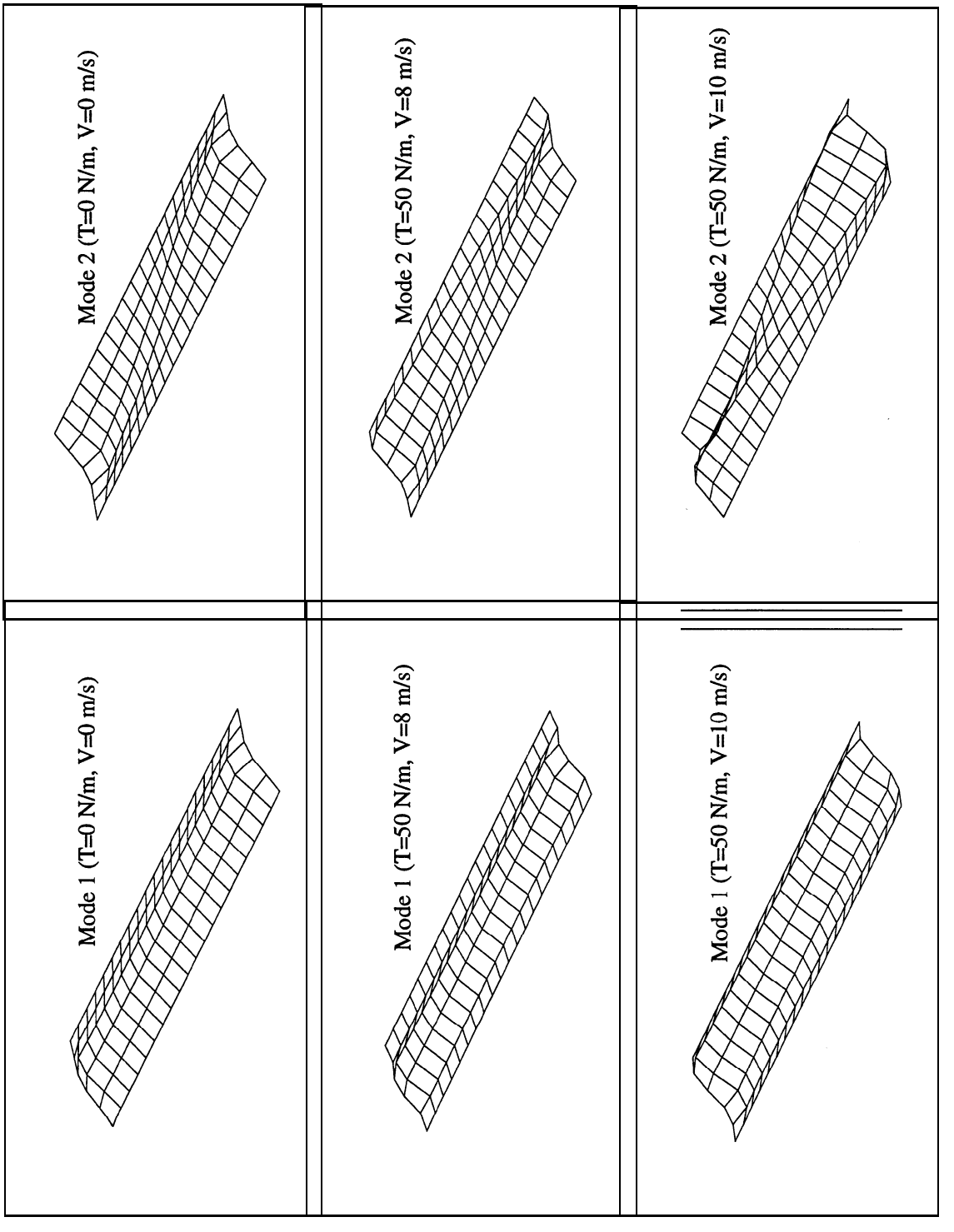

Figure 6: First two mode shapes of out-of-plane displacements. (Mesh of 5 x 20 MITC4 plate elements.)

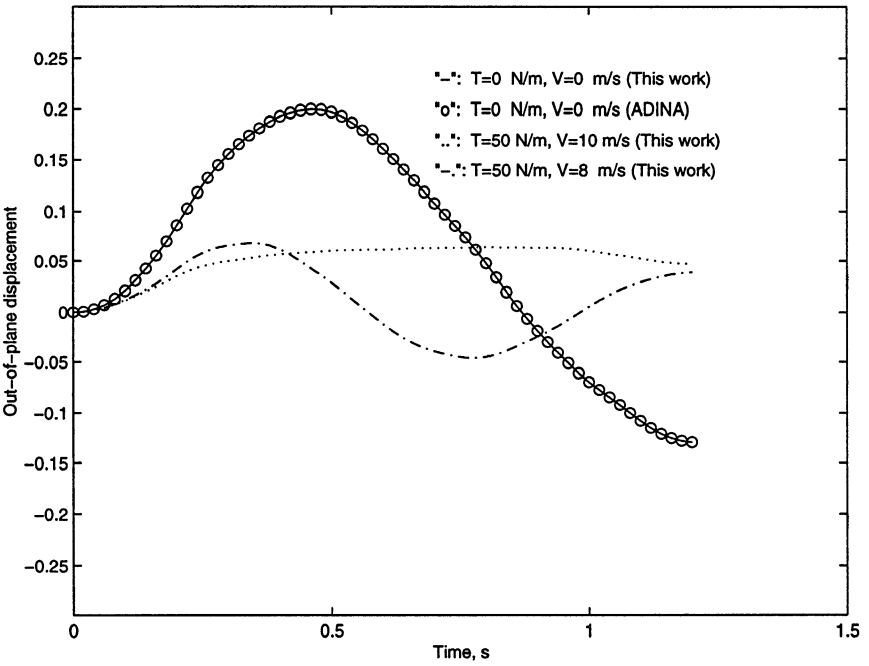

Figure 7: Out-of-plane displacement time history at the plate center.

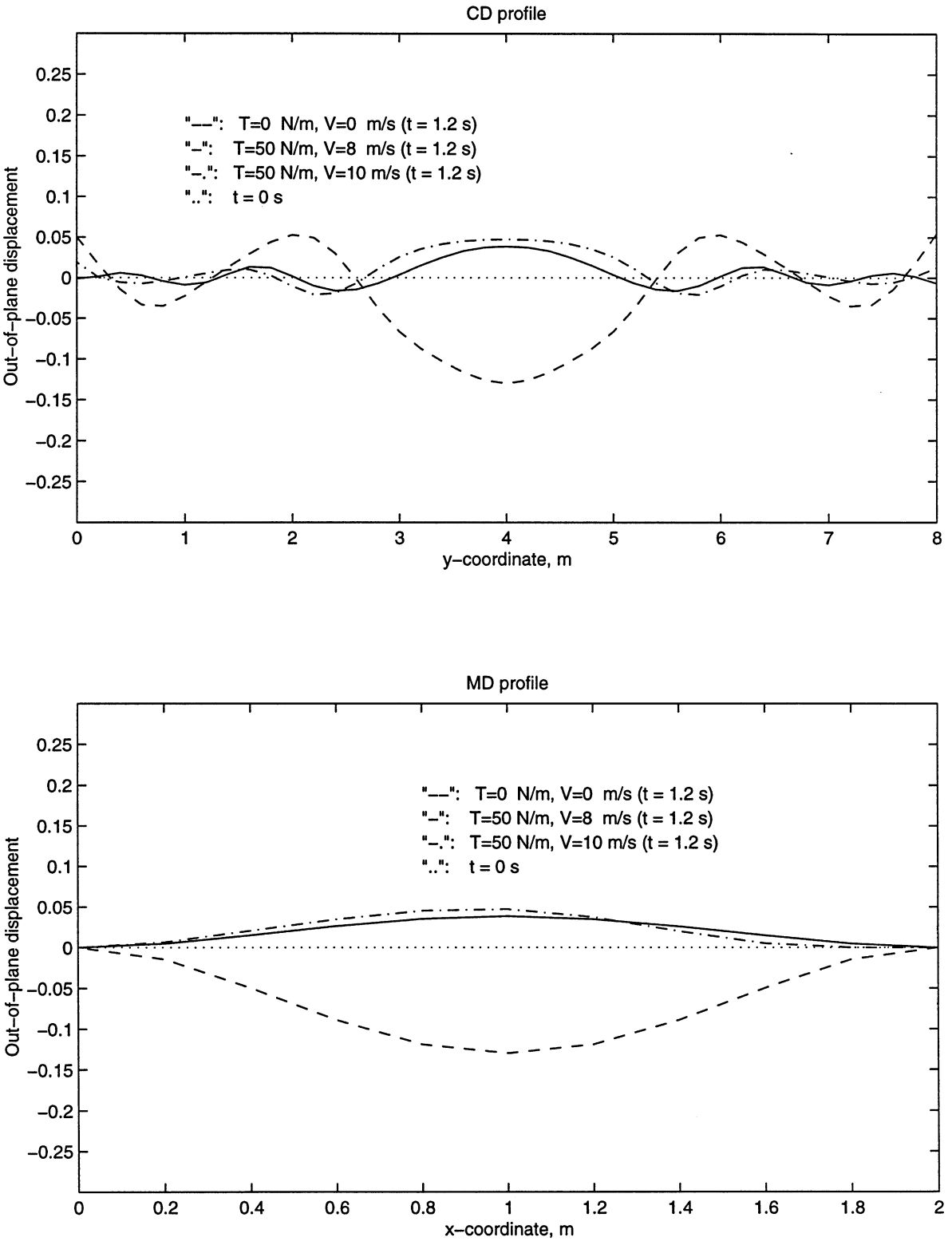

Figure 8: CD and MD out-of-plane displacement profiles for different axial velocities.

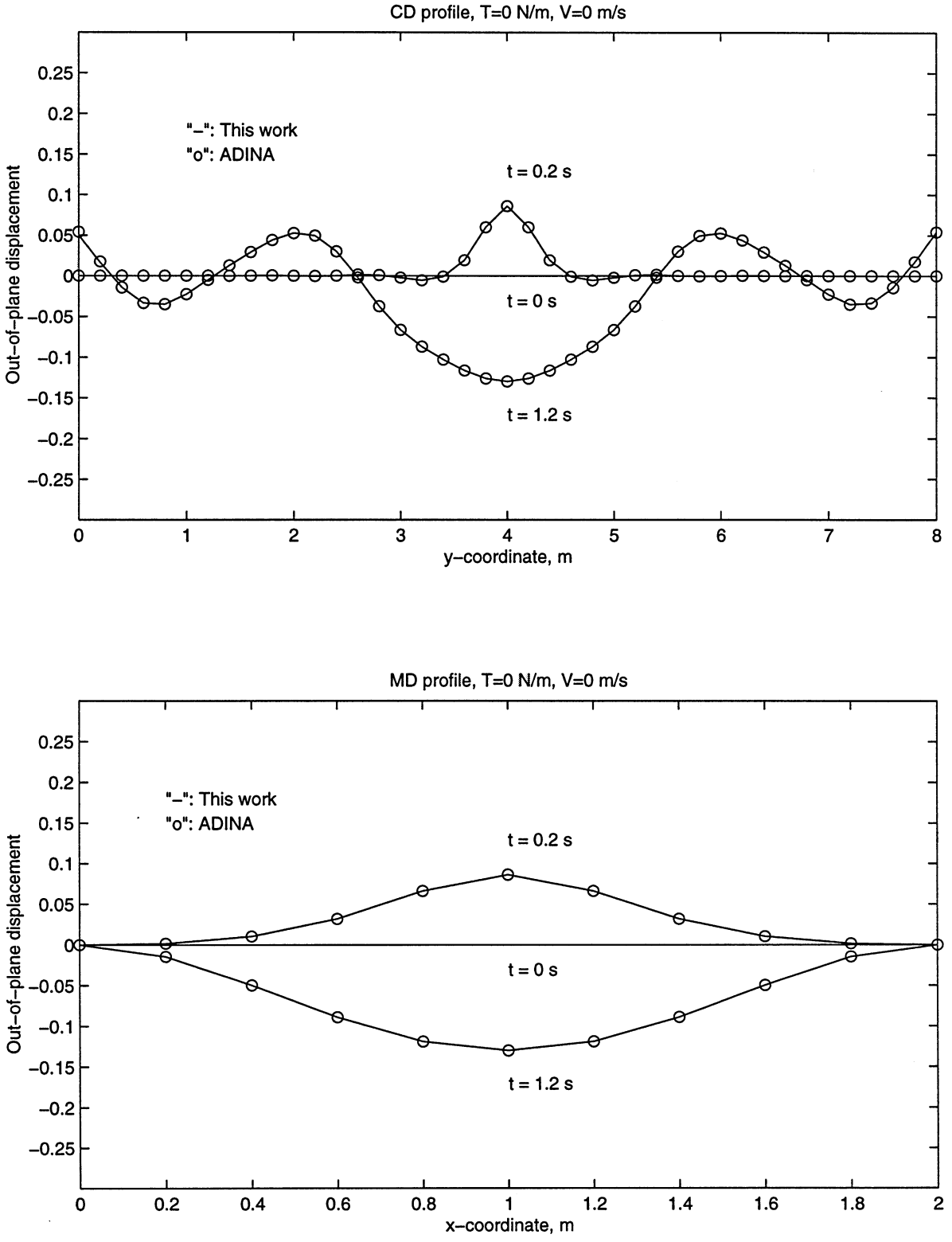

Figure 9: Comparison with ADINA of CD and MD out-of-plane displacement profiles for zero traveling velocity case.

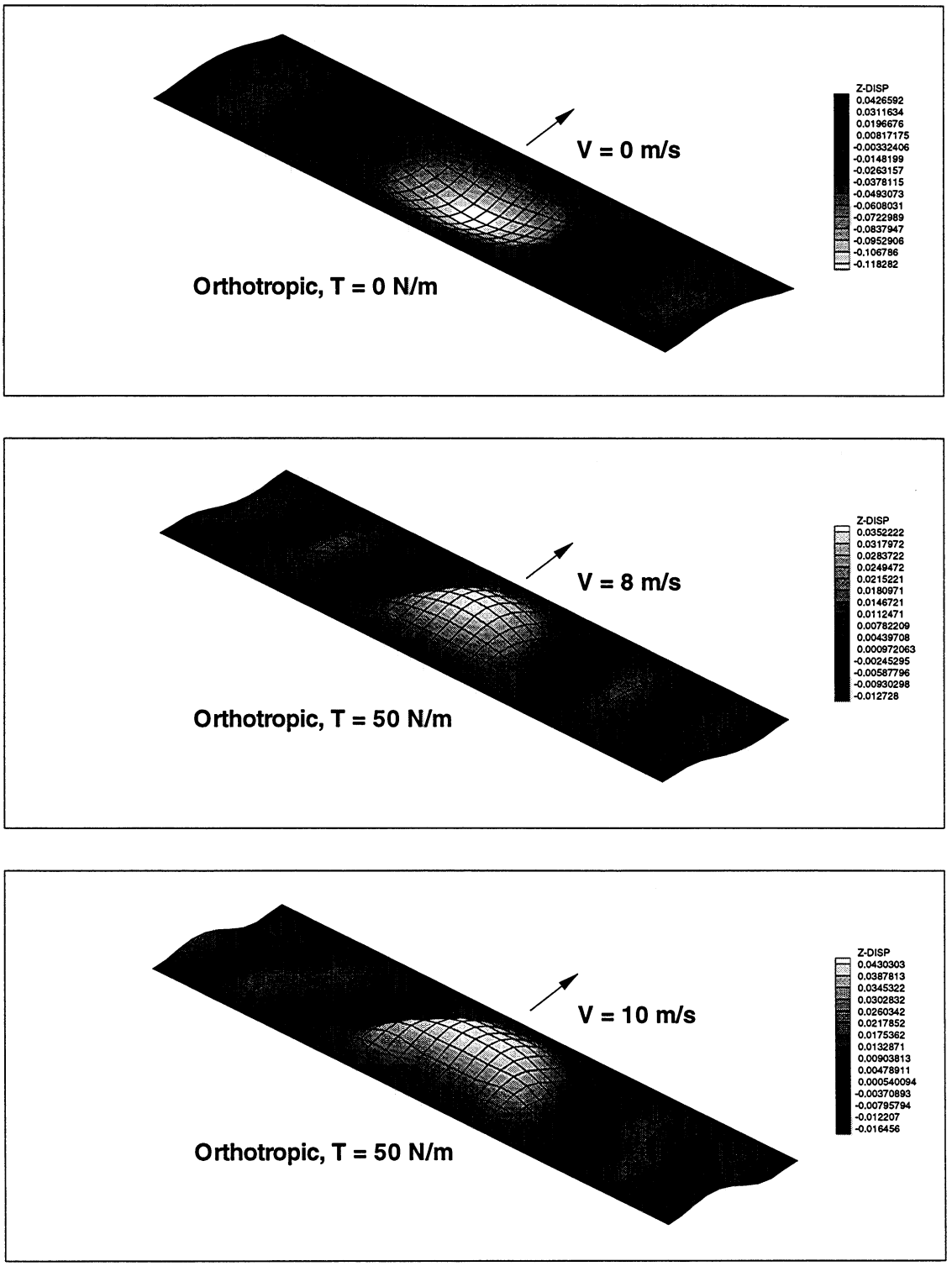

Figure 10: Out-of-plane displacement (w) bands (at $t = 1.2$ s) of the orthotropic plate moving at different velocities. (Mesh of 10×40 MITC4 plate elements.) The displacement band for zero moving velocity case is identical to ADINA results.

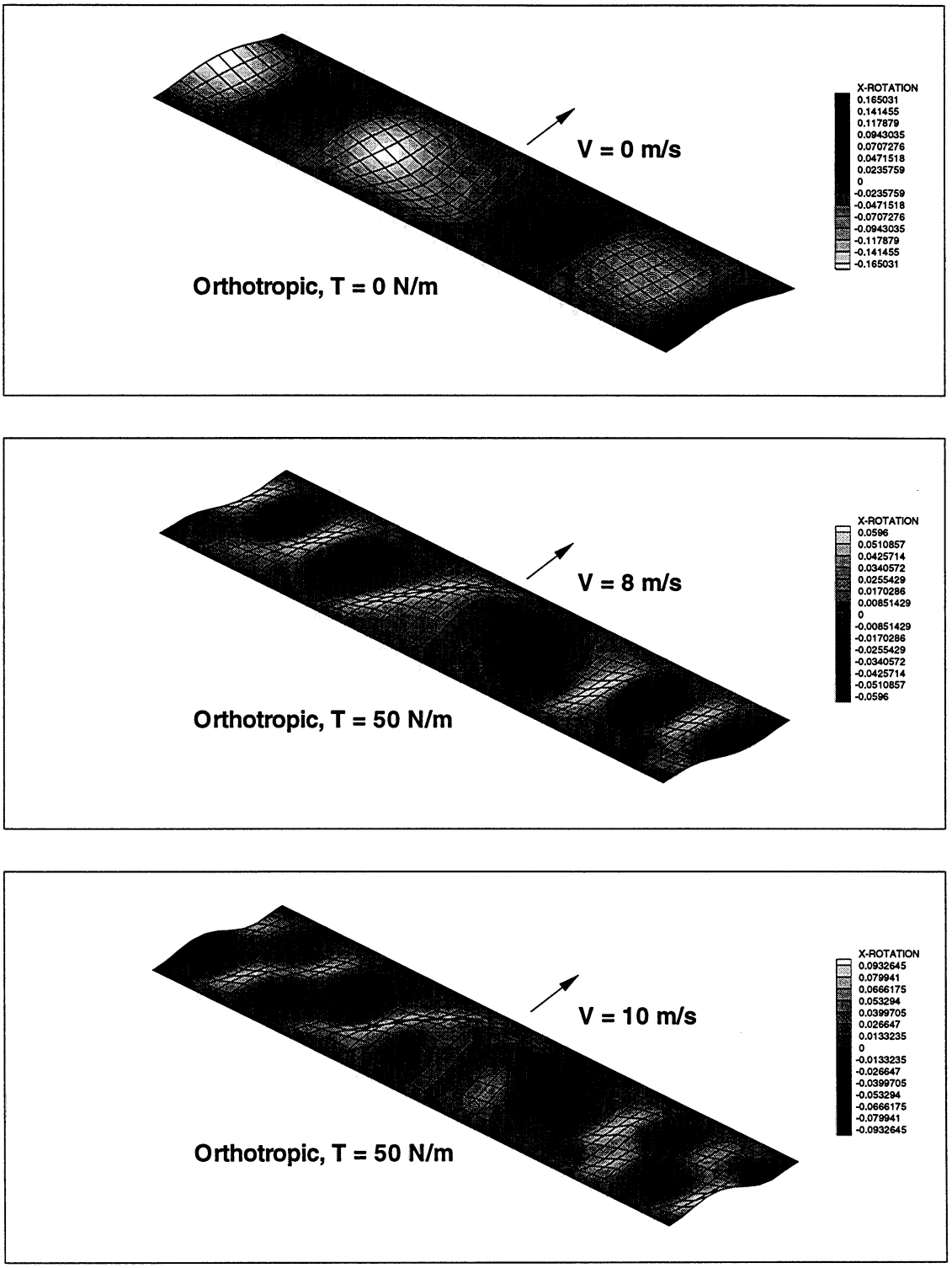

Figure 11: X direction rotation (θ_x) bands (at $t = 1.2$ s) of the orthotropic plate moving at different velocities. (Mesh of 10×40 MITC4 plate elements.) The rotation band for zero moving velocity case is identical to ADINA results.

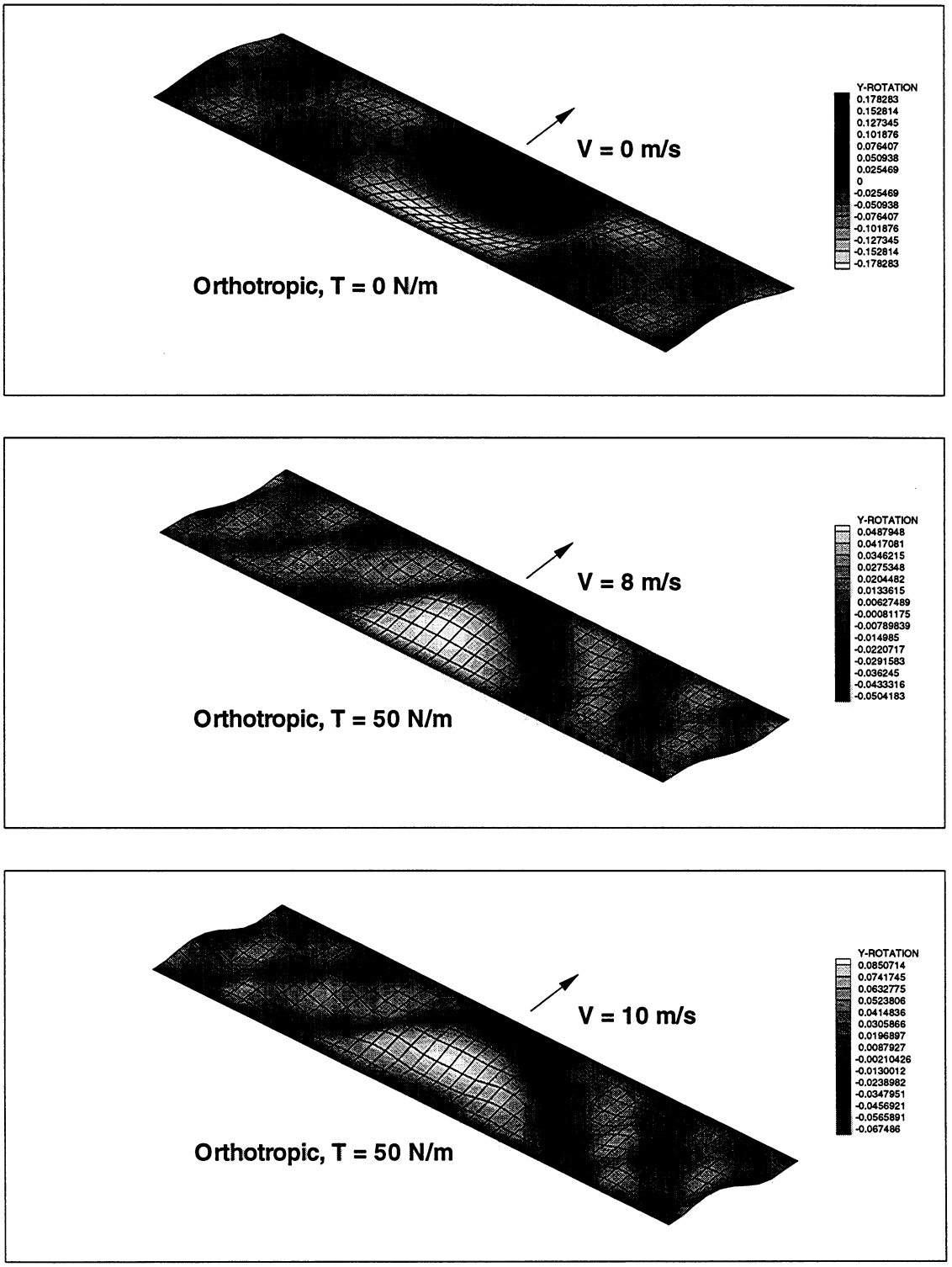

Figure 12: Y direction rotation (θ_y) bands (at $t = 1.2$ s) of the orthotropic plate moving at different velocities. (Mesh of 10×40 MITC4 plate elements.) The rotation band for zero moving velocity case is identical to ADINA results.

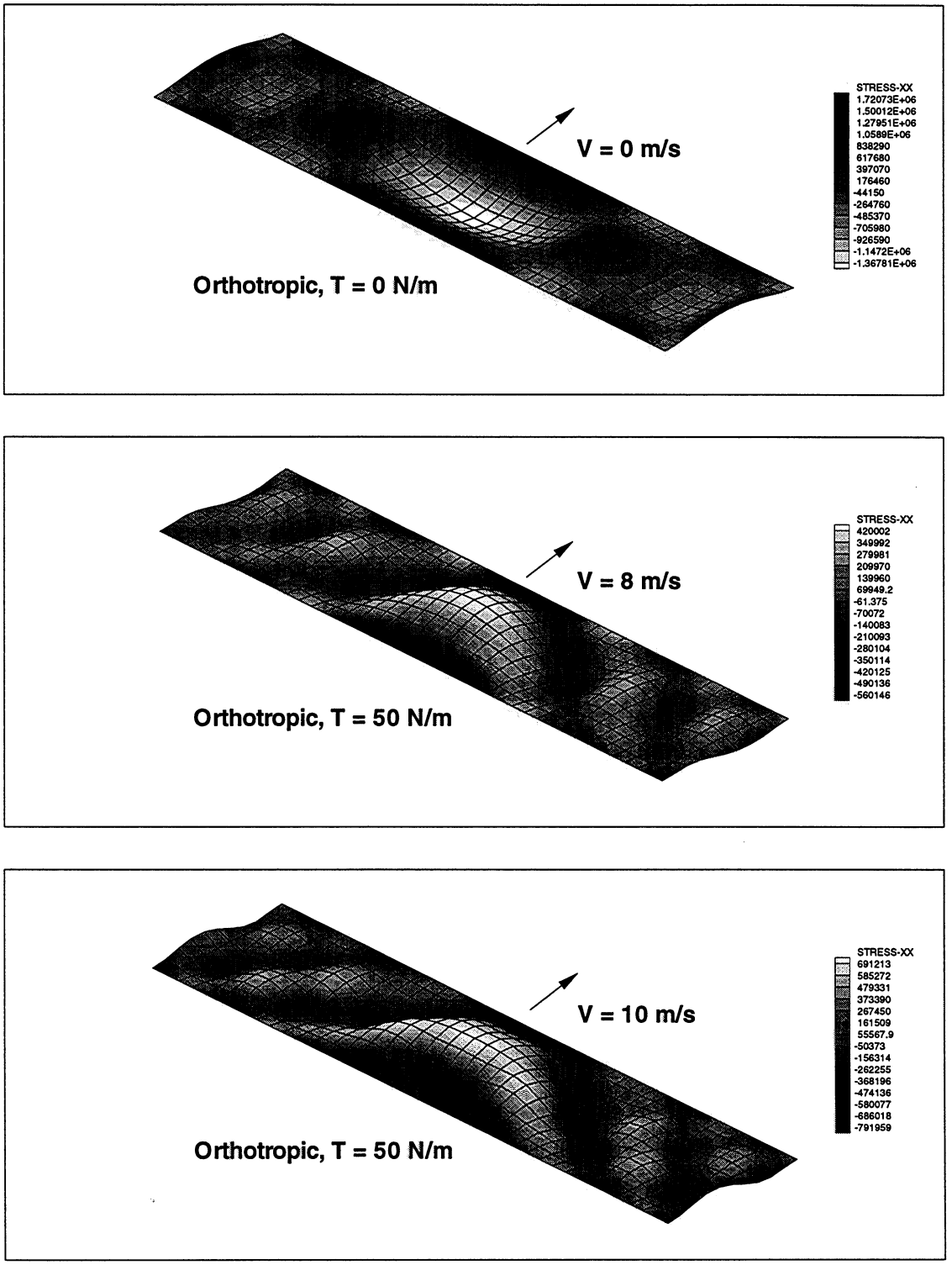

Figure 13: X direction normal stress (τ_{xx}) bands (at $t = 1.2$ s) of the orthotropic plate moving at different velocities. (Mesh of 10×40 MITC4 plate elements.) The stress band for zero moving velocity case is identical to ADINA results.

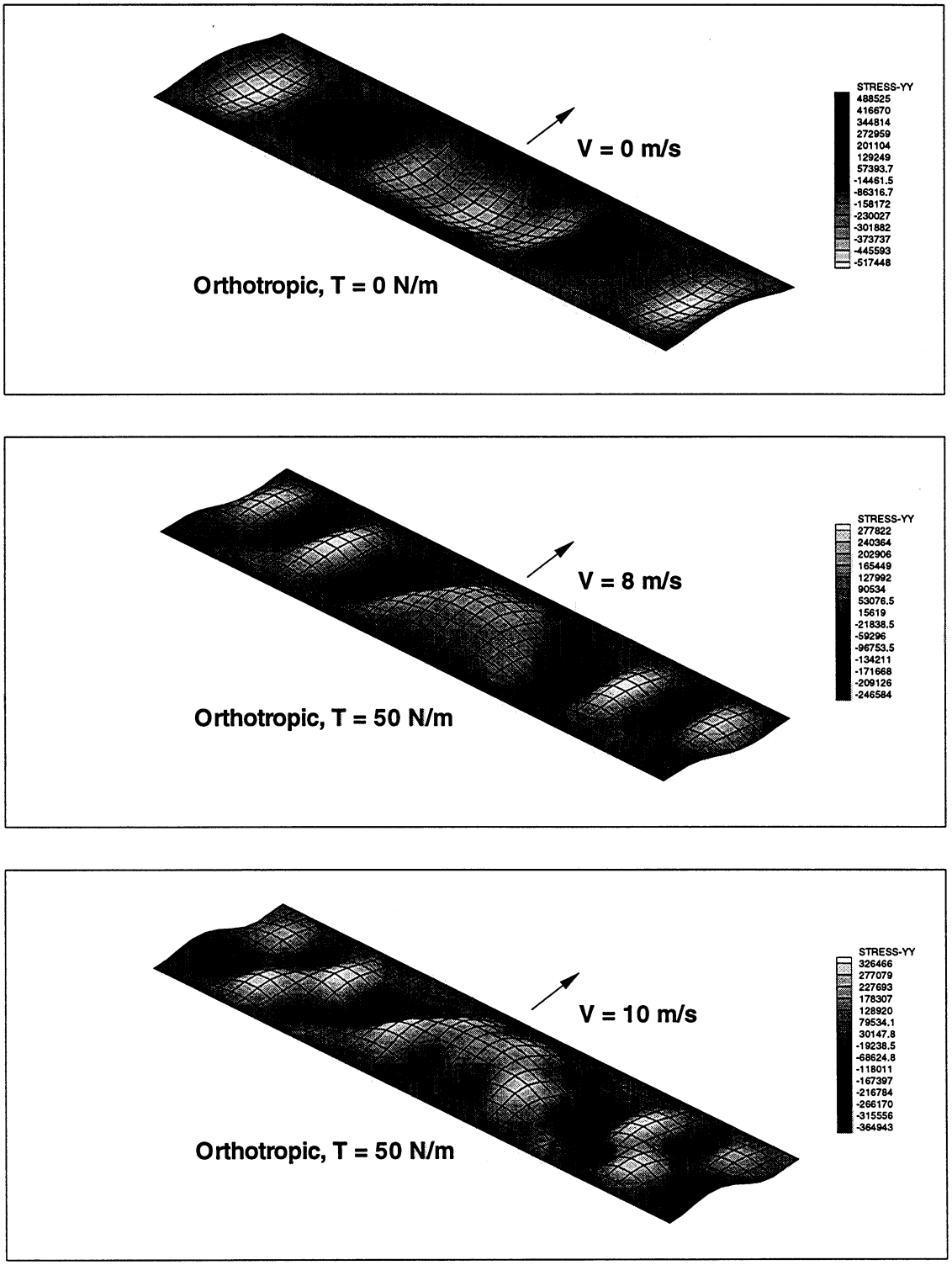

Figure 14: Y direction normal stress (τ_{yy}) bands (at $t = 1.2$ s) of the orthotropic plate moving at different velocities. (Mesh of 10×40 MITC4 plate elements.) The stress band for zero moving velocity case is identical to ADINA results.

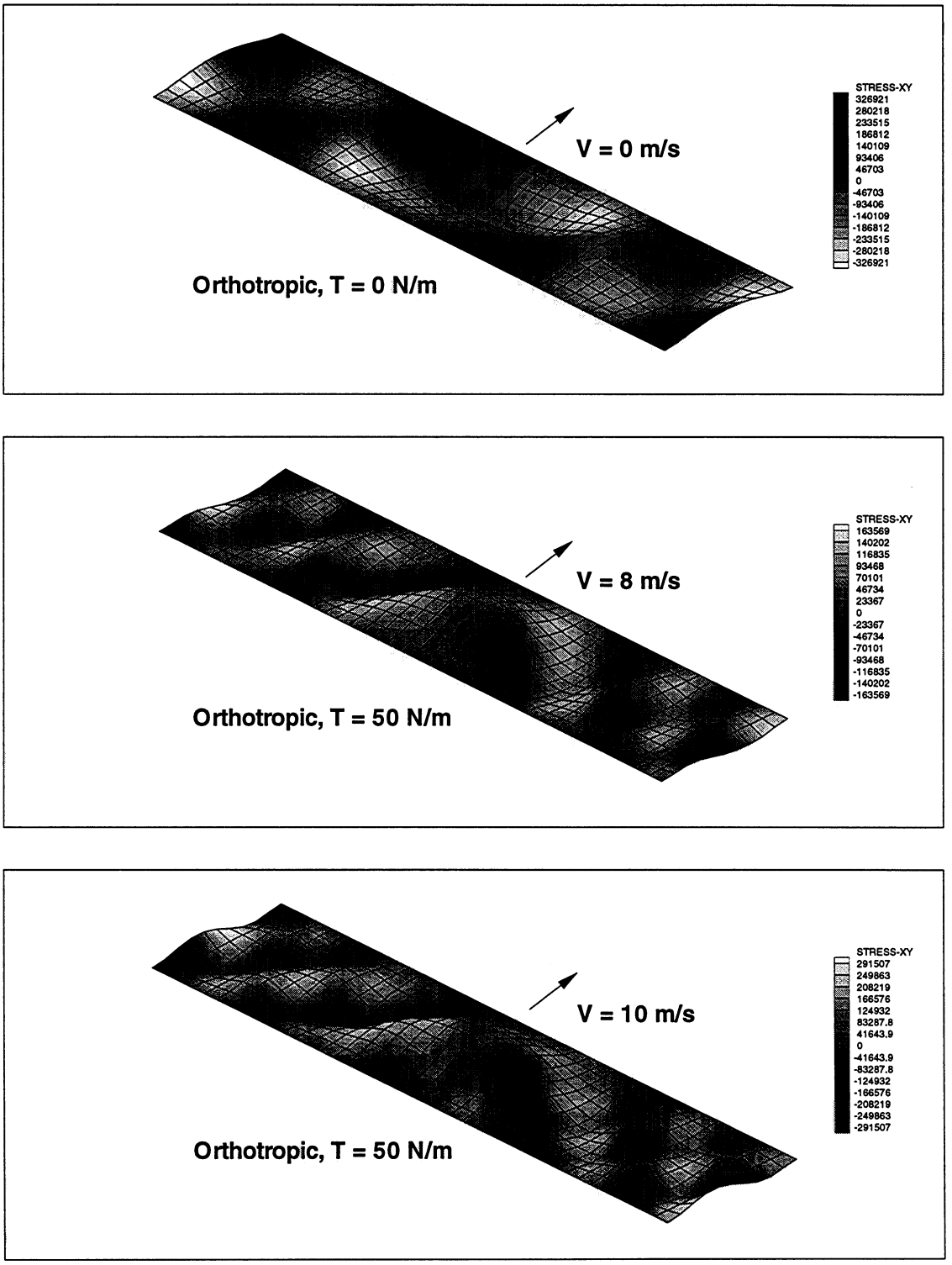

Figure 15: In-plane shear stress (τ_{xy}) bands (at $t = 1.2$ s) of the orthotropic plate moving at different velocities. (Mesh of 10×40 MITC4 plate elements.) The stress band for zero moving velocity case is identical to ADINA results.

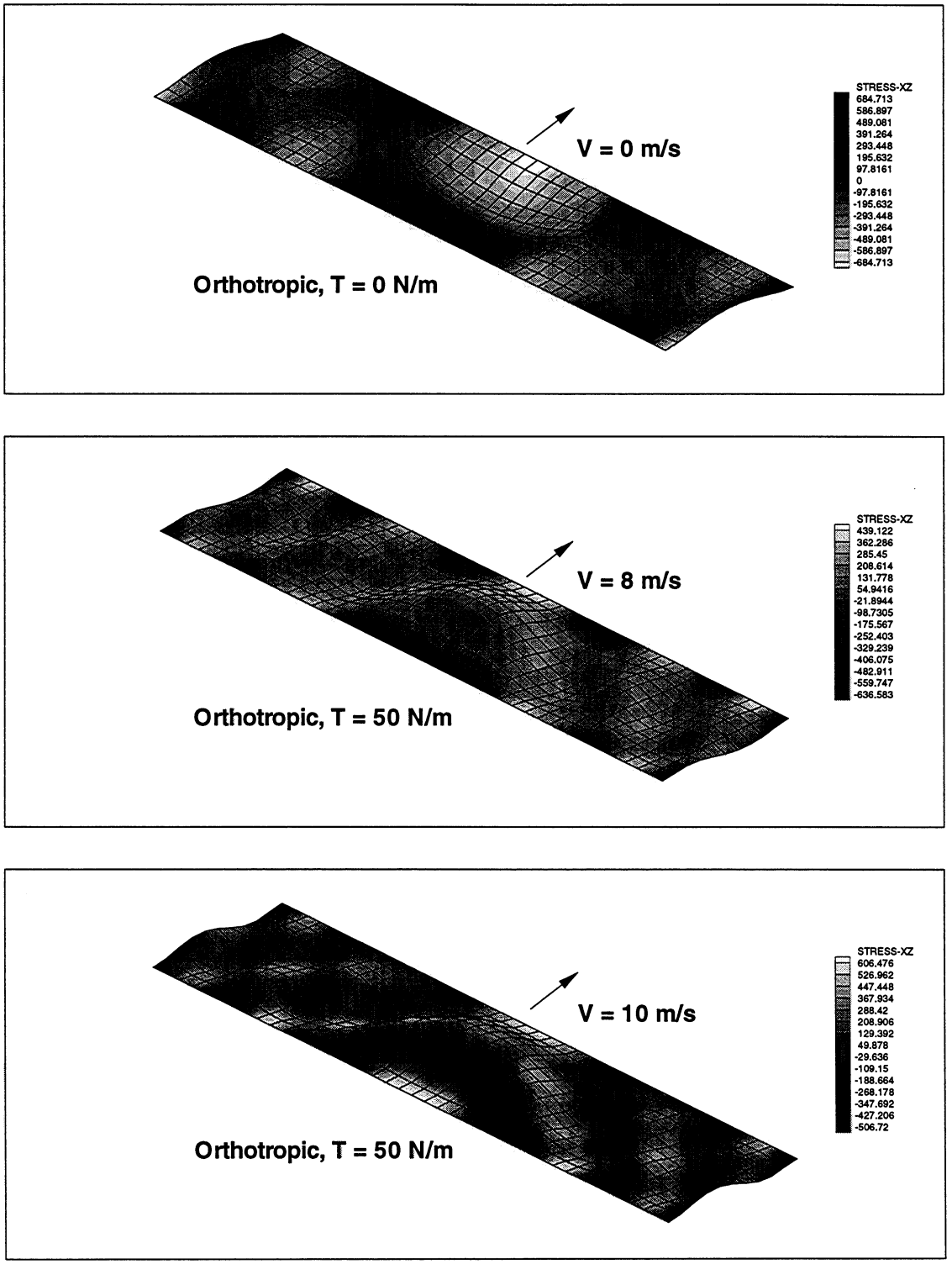

Figure 16: Transverse shear stress (τ_{xz}) bands (at $t = 1.2$ s) of the orthotropic plate moving at different velocities. (Mesh of 10×40 MITC4 plate elements.) The stress band for zero moving velocity case is identical to ADINA results.

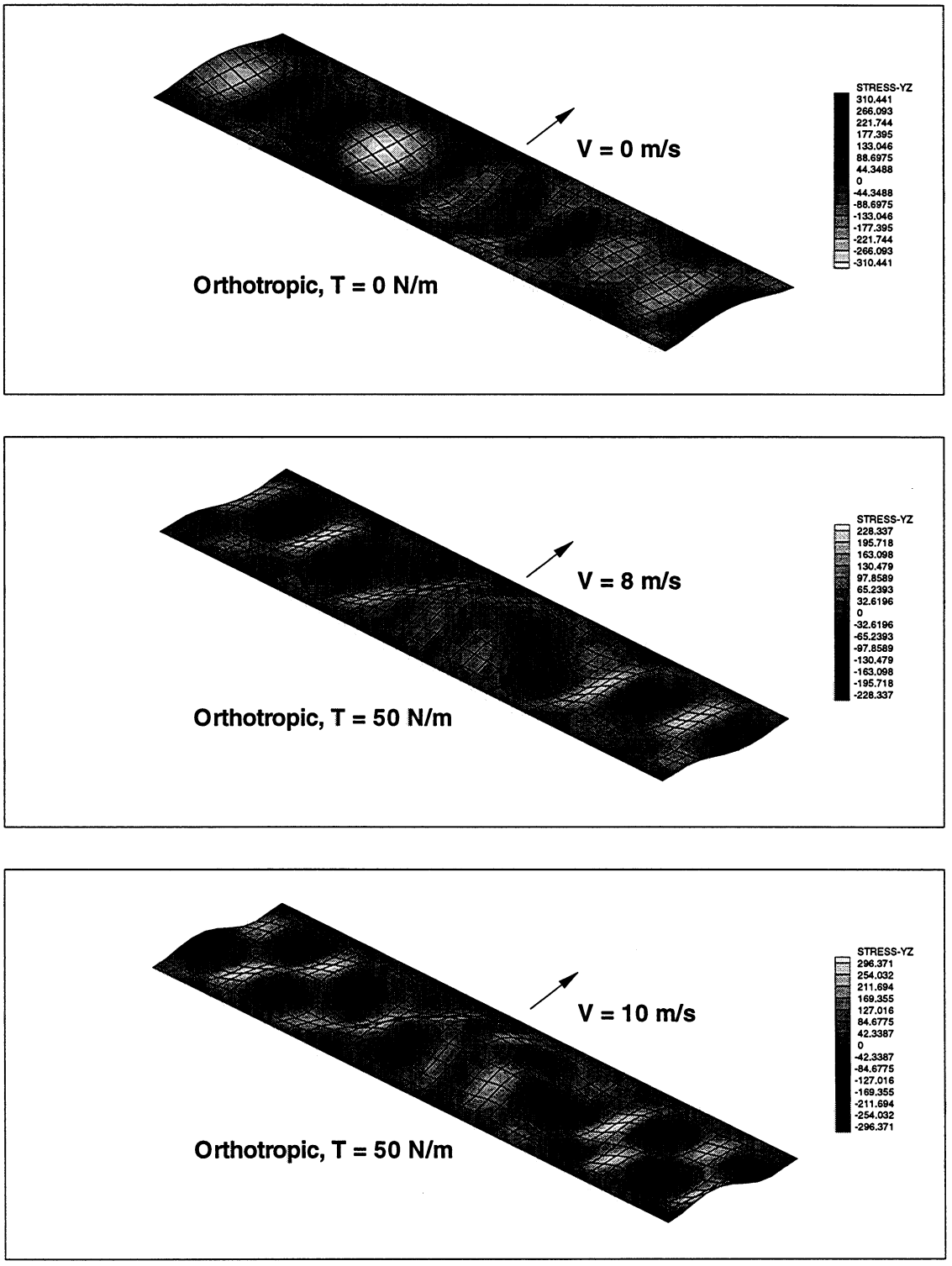

Figure 17: Transverse shear stress (τ_{yz}) bands (at $t = 1.2$ s) of the orthotropic plate moving at different velocities. (Mesh of 10×40 MITC4 plate elements.) The stress band for zero moving velocity case is identical to ADINA results.

References

[1] I. Babuška and M. Suri. The p and $h-p$ versions of the finite element method, basic principles and properties. *SIAM Review*, 36(4):578–632, 1994.

[2] K.J. Bathe. *Finite Element Procedures.* Prentice Hall, Englewood Cliffs, N.J., 1996.

[3] K.J. Bathe, M.L. Bucalem, and F. Brezzi. Displacement and stress convergence of our MITC plate bending elements. *Engineering Computation*, pages 291–302, 1990.

[4] K.J. Bathe and E.N. Dvorkin. A formulation of general shell elements-The use of mixed interpolation of tensorial components. *International Journal for Numerical Methods in Engineering*, 22:697–722, 1986.

[5] F. Brezzi, K.J. Bathe, and M. Fortin. Mixed-interpolated elements for Reissner-Mindlin plates. *International Journal for Numerical Methods in Engineering*, 28:1787–1801, 1989.

[6] J.G. Campbell. The in-plane elastic constants of paper. *Australian Journal of Applied Science*, 12:356–357, 1961.

[7] S.M. Dickinson. The buckling and frequency of flexural vibration of rectangular isotropic and orthotropic plates using Rayleigh's method. *Journal of Sound and Vibration*, 61(1):1–8, 1978.

[8] J. Dugundji, E. Dowell, and B. Perkin. Subsonic flutter of panels on continuous elastic foundations. *AIAA Journal*, pages 1146–1154, May 1963.

[9] E.N. Dvorkin and K.J. Bathe. A continuum mechanics based four-node shell element for general nonlinear analysis. *Engineering Computation*, 1:77–88, 1984.

[10] B. Häggblad and K.J. Bathe. Specifications of boundary conditions for Reissner/Mindlin plate bending finite elements. *International Journal for Numerical Methods in Engineering*, 30:981–1011, 1990.

[11] J.C. Heinrich and D. Connolly. Three-dimensional finite element analysis of self-acting foil bearings. *Computer Methods in Applied Mechanics and Engineering*, 100:31–43, 1992.

[12] H. Hencky. Über die berücksichtigung der schubverzerrung in ebenen platten. *Ingenieur Archiv*, 16:72–76, 1947.

[13] T.J.R. Hughes and T.E. Tezduyar. Finite elements based upon Mindlin plate theory with particular reference to the four-node bilinear isoparametric element. *Journal of Applied Mechanics*, 48:587–596, 1981.

[14] A. Iosilevich, K.J. Bathe, and F. Brezzi. On evaluating the Inf-Sup condition for plate bending elements. *International Journal for Numerical Methods in Engineering*, 1997. To appear.

[15] C.A. Lacey and F.E. Talke. A tightly coupled numerical foil bearing solution. *IEEE Transactions on Magnetics*, 26(6):3039–3043, November 1990.

[16] H.P. Lee and T.Y. Ng. Transverse vibration of a plate moving over multiple point supports. *Applied Acoustics*, 47(4):291–301, 1996.

[17] R.D. Mindlin. Influence of rotatory inertia and shear on flexural motions of isotropic, elastic plates. *Journal of Applied Mechanics*, pages 31–38, 1951.

[18] C.D. Mote. A study of band saw vibrations. *Journal of the Franklin Institute*, 279(6):430–444, 1965.

[19] S. Müftü and R.C. Benson. Modelling the transport of paper webs including the paper permeability effects. *Proceedings of ISPS at the ASME-International Congress and Exposition in San Fransisco, CA*, November 1995.

[20] Y.D. Murray and C.D. Mote, Jr. Analysis of a plane inclined guide bearing under transverse vibration and translation of a plate. *Journal of Lubrication Technology*, 105:335–341, 1983.

[21] A. Pramila. Natural frequencies of a submerged axially moving band. *Journal of Sound and Vibration*, 113(1):198–203, 1987.

[22] E. Reissner. The effect of transverse shear deformation on the bending of elastic plates. *Journal of Applied Mechanics*, pages (A)69–77, June 1945.

[23] R. Stenberg and M. Suri. An *hp* error analysis of MITC plate elements. *SIAM Journal of Numerical Analysis*, 34(2):544–568, 1997.

[24] M. Suri, I. Babuška, and C. Schwab. Locking effects in the finite element approximation of plate models. *Mathematics of Computation*, 64(210):461–482, 1995.

[25] C.A. Tan and C.D. Mote, Jr. Analysis of a hydrodynamic bearing under transverse vibration of an axially moving band. *Journal of Tribology*, 112:514–523, 1990.

[26] S. Timoshenko and S. Woinowsky-Krieger. *Theory of Plates and Shells.* McGraw-Hill Publishing Company, second edition edition, 1987.

[27] S.P. Timoshenko. On the transverse vibrations of bars of uniform cross section. *Philosophical Magazine*, 43(A):125–131, 1922.

[28] Ya.S. Uflyand. The progagation of waves in the transverse vibrations of bars and plates. *Prikl. Mat. Meh.*, 12:287–300, 1948.

[29] X. Wang. Finite element analysis of air-sheet interactions and flutter suppression devices. *Computers & Structures*, 64(5/6):983–994, 1997.

[30] X. Wang and G. Renner. Computational simulation of three-dimensional pretensioned moving paper webs. *Nineteenth Southeastern Conference on Theoretical and Applied Mechanics*, May 1998. In press.

[31] J.A. Wickert. Non-linear vibration of a traveling tensioned beam. *International Journal of Non-linear Mechanics*, 27(3):503–517, 1992.

[32] J.A. Wickert and C.D. Mote, Jr. Current research on the vibration and stability of axially moving materials. *The Shock and Vibration Digest*, 20:3–13, 1988.

[33] J.A. Wickert and C.D. Mote, Jr. Classical vibration analysis of axially moving continua. *Journal of Applied Mechanics*, 57:738–744, 1990.

[34] B. Yang and C.D. Mote, Jr. Active vibration control of the axially moving string in the s domain. *Journal of Applied Mechanics*, 58:189–196, 1991.